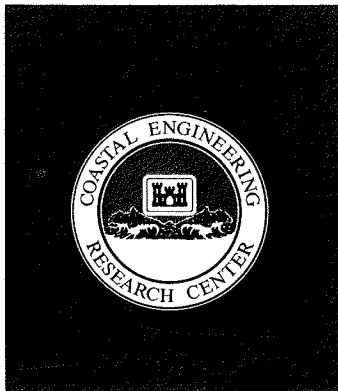
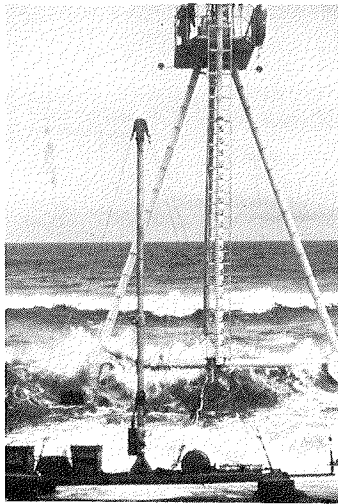
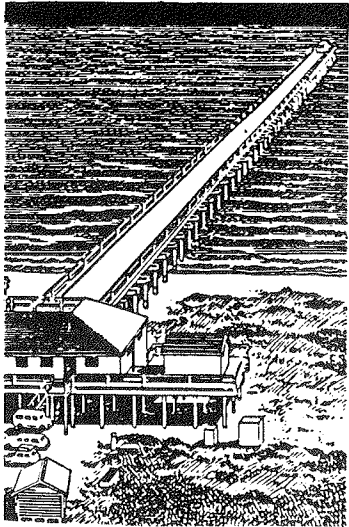




**US Army Corps
of Engineers**



TECHNICAL REPORT CERC-90-17

COMPARISON OF ATLANTIC COAST WAVE INFORMATION STUDY HINDCASTS WITH FIELD RESEARCH FACILITY GAGE MEASUREMENTS

by

Herman C. Miller, Robert E. Jensen

Coastal Engineering Research Center

DEPARTMENT OF THE ARMY

Waterways Experiment Station, Corps of Engineers
3909 Halls Ferry Road, Vicksburg, Mississippi 39180-6199



October 1990

Final Report

Approved For Public Release; Distribution Unlimited

Prepared for DEPARTMENT OF THE ARMY
US Army Corps of Engineers
Washington, DC 20314-1000

Under Work Unit 32525

**Destroy this report when no longer needed. Do not return
it to the originator.**

**The findings in this report are not to be construed as an official
Department of the Army position unless so designated
by other authorized documents.**

**The contents of this report are not to be used for
advertising, publication, or promotional purposes.
Citation of trade names does not constitute an
official endorsement or approval of the use of
such commercial products.**

Unclassified

SECURITY CLASSIFICATION OF THIS PAGE

REPORT DOCUMENTATION PAGE				Form Approved OMB No. 0704-0188	
1a. REPORT SECURITY CLASSIFICATION Unclassified		1b. RESTRICTIVE MARKINGS			
2a. SECURITY CLASSIFICATION AUTHORITY		3. DISTRIBUTION/AVAILABILITY OF REPORT Approved for public release; distribution unlimited.			
2b. DECLASSIFICATION/DOWNGRADING SCHEDULE					
4. PERFORMING ORGANIZATION REPORT NUMBER(S) Technical Report CERC-90-17			5. MONITORING ORGANIZATION REPORT NUMBER(S)		
6a. NAME OF PERFORMING ORGANIZATION USAEWES, Coastal Engineering Research Center		6b. OFFICE SYMBOL (if applicable)	7a. NAME OF MONITORING ORGANIZATION		
6c. ADDRESS (City, State, and ZIP Code) 3909 Halls Ferry Road Vicksburg, MS 39180-6199			7b. ADDRESS (City, State, and ZIP Code)		
8a. NAME OF FUNDING/SPONSORING ORGANIZATION US Army Corps of Engineers		8b. OFFICE SYMBOL (if applicable)	9. PROCUREMENT INSTRUMENT IDENTIFICATION NUMBER		
8c. ADDRESS (City, State, and ZIP Code) Washington, DC 20314-1000			10. SOURCE OF FUNDING NUMBERS		
	PROGRAM ELEMENT NO.	PROJECT NO.	TASK NO.	WORK UNIT ACCESSION NO. 32525	
11. TITLE (Include Security Classification) Comparison of Atlantic Coast Wave Information Study Hindcasts with Field Research Facility Gage Measurements					
12. PERSONAL AUTHOR(S) Miller, Herman C.; Jensen, Robert E.					
13a. TYPE OF REPORT Final report		13b. TIME COVERED FROM _____ TO _____	14. DATE OF REPORT (Year, Month, Day) October 1990		15. PAGE COUNT 36
16. SUPPLEMENTARY NOTATION Available from National Technical Information Service, 5285 Port Royal Road, Springfield, VA 22161.					
17. COSATI CODES			18. SUBJECT TERMS (Continue on reverse if necessary and identify by block number)		
FIELD	GROUP	SUB-GROUP	See reverse.		
19. ABSTRACT (Continue on reverse if necessary and identify by block number)					
<p>One of the most comprehensive compilations of wave information is the hindcast wave estimates provided by the US Army Corps of Engineers' Wave Information Studies (WIS). This report compares summaries of the 1956-1975 Atlantic coast Phase III shallow-water WIS estimates with two measured data sets from the Coastal Engineering Research Center's Field Research Facility (FRF) at Duck, NC. The first consists of 5 years of energy spectra from a Waverider buoy, while the second is 1 year of directional spectra from a high-resolution linear array. Results of the study provide the engineer with a clear understanding of the differences between the WIS estimates and the FRF measurements that will help ensure the appropriate application of the WIS wave information.</p>					
(Continued)					
20. DISTRIBUTION/AVAILABILITY OF ABSTRACT <input checked="" type="checkbox"/> UNCLASSIFIED/UNLIMITED <input type="checkbox"/> SAME AS RPT. <input type="checkbox"/> DTIC USERS			21. ABSTRACT SECURITY CLASSIFICATION Unclassified		
22a. NAME OF RESPONSIBLE INDIVIDUAL		22b. TELEPHONE (Include Area Code)		22c. OFFICE SYMBOL	

18. SUBJECT TERMS (Continued).

Average wave period	Wave direction
Field Research Facility (FRF)	Wave height
Linear array	Wave hindcasts
Longshore sediment transport rate	Wave Information Studies (WIS)
Peak spectral wave period	Waverider buoy

19. ABSTRACT (Continued).

Following a description of the WIS estimates and the FRF measurements, wave period, height, and direction summaries are compared. The wave periods did not compare well, whereas wave heights did. The wave direction comparison is less conclusive; however, net longshore sediment transport estimates made using the WIS estimates are very close to that using the FRF measurements.

An attempt is made to reconcile the differences in the wave periods with only limited success. In addition to the use of different definitions of period, it is suggested that questions about wave generation and propagation will have to be answered before close agreement can be expected.

Wave height distributions agree well for waves over 2 m. However, only 44 percent of the heights exceed 0.5 m for the WIS estimates, compared with 76 percent for the FRF measurements. This difference is attributed, in part, to the coastal orientation, which greatly reduces the fetch for winds blowing near shore-parallel at the gage site. Also, the Phase III hindcast method does not consider additional wind-wave growth from the input Phase II points.

Both the WIS and FRF directions tend to be primarily shore-normal. A clear difference between the distributions is that the WIS estimates have many more shore-parallel low waves. This difference arises because the hindcast method allows for the transformation of wind-sea energy derived from wave conditions propagating in all directions.

Longshore sediment transport rate estimates are computed to investigate the consistency between using the WIS estimates versus the FRF measurements for engineering applications. Although the gross northward and southward values differed by as much as a factor of 2, the net values are very similar. When annual gross northerly and southerly values for each of the 20 years of WIS estimates are compared with the FRF measurements, the FRF transport rates fall well within the variation of the WIS estimates. The consistency in the WIS estimates is due in part to the transport rate computation being more sensitive to wave height and direction, for which WIS estimates and FRF measurements generally agree, versus wave period for which the WIS estimates are low.

PREFACE

Authority for the US Army Engineer Waterways Experiment Station's (WES's) Coastal Engineering Research Center (CERC) to conduct this study was granted by the Headquarters, US Army Corps of Engineers (HQUSACE), under Work Unit 32525, "FRF Analysis," Coastal Flooding and Shore Protection Program, Coastal Engineering Area of Civil Works Research and Development. The HQUSACE Technical Monitors for this research were Messrs. John H. Lockhart, Jr.; John G. Housley; James E. Crews; and Charles W. Hummer. The CERC Program Manager was Dr. C. Linwood Vincent.

The study was conducted by Mr. Herman C. Miller, Field Research Facility (FRF), Engineering Development Division (EDD), and Dr. Robert E. Jensen, Coastal Oceanography Branch (COB), Research Division (RD), CERC. Mr. Miller's work was carried out under the direct supervision of Mr. William A. Birkemeier, Chief, FRF, and Mr. Thomas W. Richardson, Chief, EDD; Dr. Jensen's work was carried out under the direct supervision of Dr. Martin C. Miller, Chief, COB, and Mr. H. Lee Butler, Chief, RD; and under the general supervision of Dr. James R. Houston and Mr. Charles C. Calhoun, Jr., Chief and Assistant Chief, CERC, respectively.

COL Larry B. Fulton, EN, was Commander and Director during publication of this report. Dr. Robert W. Whalin was Technical Director.

CONTENTS

	<u>Page</u>
PREFACE	1
PART I: INTRODUCTION	3
Background	3
Scope and Purpose of Study	4
PART II: WAVE HINDCASTS AND MEASUREMENTS	7
WIS Hindcasts	7
FRF Measurements	10
PART III: COMPARISON OF WIS TO FRF	13
Percent Occurrence Tables	13
Wave Period	13
Wave Height	20
Wave Direction	21
Summary	23
PART IV: LONGSHORE SEDIMENT TRANSPORT ESTIMATE	24
PART V: SUMMARY	29
REFERENCES	31

COMPARISON OF ATLANTIC COAST WAVE INFORMATION STUDY HINDCASTS
WITH FIELD RESEARCH FACILITY GAGE MEASUREMENTS

PART I: INTRODUCTION

Background

1. According to Wang and Lé Mehauté (1983), ". . . short-term wave measurements of a few years are not sufficient for engineering accuracy, and can be used only to verify or complement wave height estimation given by other methods such as hindcasting." Their study shows statistically that the uncertainties in extrapolations of wave information to large return intervals decrease as the number of years of data increases. Historically, wave measurements have been for short times in comparison to the 20 to 30 years required for reasonable confidence in extrapolations to 50- or 75-year return intervals. Also, in the past, wave measurements have been available from only a few selected locations along the US coasts (Thompson 1977). Although wave measurements have been made at many more locations during the past decade and new gage locations are being added each year as part of a national Coastal Field Data Collection (Hemsley 1986), the long-term measurements necessary for accurate engineering design are decades away.

2. Until then, the engineer must rely on other sources of wave data. One of the most comprehensive compilations of wave information is the hindcast wave estimates provided by the US Army Corps of Engineers' Wave Information Studies (WIS). In a series of 19 reports to date, 20 years of deep-, intermediate-, and shallow-water wave height, period, and direction estimates for the Atlantic, Gulf of Mexico, Pacific, and Great Lakes coasts of the United States are provided.

3. Although the shallow-water hindcasts, which are computed for approximately 16-km (10 nautical mile) intervals, are much less expensive (and about 19 years quicker to obtain) than a 20-year measurement program, both the computational procedures and the parameters selected for dissemination were optimized to minimize the cost of obtaining long-term wave height, period, and direction information along the US coastline (Jensen 1983a). Extensive efforts have been made to use state-of-the-art methodology for the problem of accurately computing winds and waves over large ocean areas from historical

meteorological records and subsequently transforming this information into shallow water. However, since many questions regarding the generation and propagation of wave energy remain unanswered, any model that is used will not reproduce all the natural conditions exactly.

4. The engineer is therefore faced with a decision because both sources of wave information have trade-offs. On the one hand, the WIS estimates provide the largest number of years of wave information. This should increase the confidence in any extrapolations that are required. The data are also available along the entire coastline. However, are the hindcasting methods sufficiently accurate to reproduce the wave conditions? On the other hand, does the accuracy of the gage measurements justify the statistical inaccuracy possible from using a much shorter data set at only selected sites? It is difficult to answer these questions due to insufficient measurements of actual conditions to compare with the hindcasts. The best that can be done is to compare the hindcasts and measurements for the few locations where measurements are available to see how well they agree and then to use "engineering judgment."

Scope and Purpose of Study

5. Corson and Resio (1981) and Jensen (1983b) compared wave height and period values for the Atlantic coast hindcasts on a case-by-case basis with data from the few available gage locations and determined that they were quite similar to the measured data. Unfortunately, directional wave measurements were not available for the gage locations used for the comparisons. This report presents a hindcast evaluation that includes shallow-water directional wave information. Since the measurements do not overlap the dates of the hindcasts, a case-by-case comparison is not possible. However, the long-term, comprehensive measurement program at the US Army Engineer Waterways Experiment Station (WES), Coastal Engineering Research Center's Field Research Facility (FRF) located on the Outer Banks of North Carolina near Duck, NC (Figure 1), provides an opportunity to compare wave climate characteristics, including wave direction. The results provided will give the engineer a clear understanding of the differences between the shallow-water, Atlantic coast summary statistics provided in WIS Report 9 and the gage measurements from the FRF (Miller et al. 1988; and Long and Oltman-Shay, in preparation).

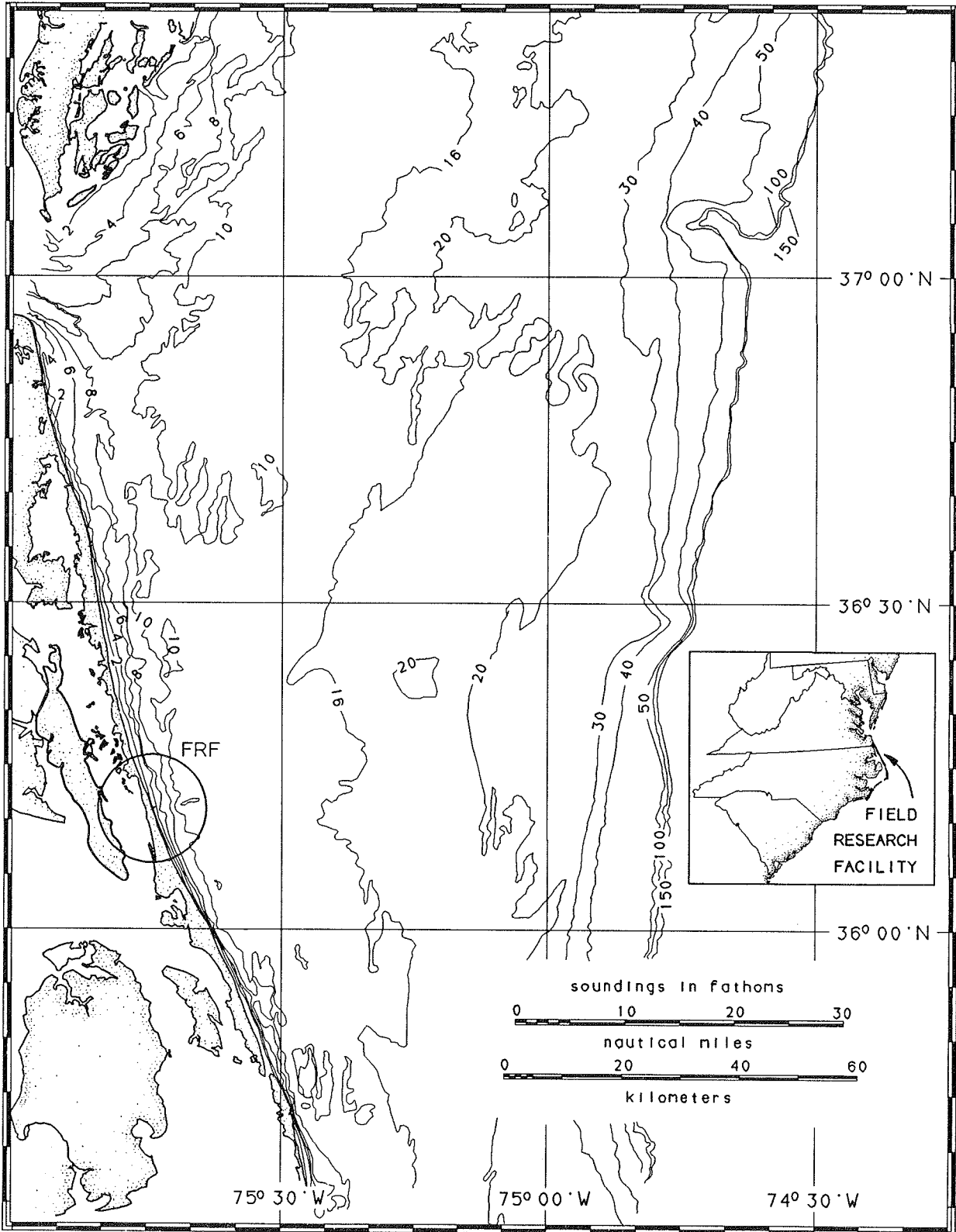


Figure 1. Location of FRF and offshore bathymetry

6. The FRF has a typical marine climate. Winds are generally from the southwest during the spring and summer switching to predominantly northerly during autumn and winter. The annual mean wave height and period at the seaward end of the FRF pier (depth 8 m) are 1 m (0.6-m standard deviation) and 8 sec (2-sec standard deviation), respectively. Tide range is 1 m, and the nearshore bathymetry is characterized by regular shore-parallel contours, a moderate slope, and a barred surf zone (usually an outer bar in water depths of about 4.5 m and an inner bar in water depths between 1.0 and 2.0 m).

7. This report is organized such that a description of the WIS estimates and FRF measured wave statistics follows in Part II. Next, the wave height, period, and direction distributions are compared for the 20-year hindcasts and measured data (Part III). Following the wave statistics comparison, the reader will find an example of how the results of estimating longshore sediment transport rates using the hindcast wave information compares with the same computation using measured wave data (Part IV). Conclusions of the report findings are provided in Part V.

9. Phases I and II were generated in a time-dependent mode. A discrete spectral wave model was employed (Resio 1981) where wind-wave growth, non-linear wave-wave interactions, and propagation were the main mechanisms modeled. This method propagated two-dimensional (2-D) (frequency and direction space) spectral estimates over the gridded system in time.

10. In the deepwater wave hindcasts, 20 discrete frequency increments and 16 discrete angle increments were used to approximate continuous 2-D wave spectra (Resio 1981). If all 320 elements in the 16 by 20 array were treated as independent, the number of calculations for each wave transformation into shallow water would become ridiculously large for the computer resources at that time. If the spectra were reduced to simple monochromatic wave trains, significant information pertaining to the randomness of the ocean surface characterized by a spectrum would be lost.

11. Thus, a totally different approach from Phases I and II was used in the generation of wave information in the nearshore region of Phase III. Using Phase II results as input, spectral refraction and shoaling were introduced in the Phase III method (Jensen 1983b). This method assumes that the bottom contours are straight and parallel and that no additional source is present, which also implies that the wave period is held fixed. By assuming plane beach conditions and the transformation from deep to a predetermined water depth of 10-m, a spatial or time marching solution method was not needed. All shoaling and refraction processes could be determined in a single step, without a loss in accuracy. It was also determined that nonlinear wave-wave interactions control the relative amount of energy losses when the spectrum approached shallow water and thus bottom frictional effects were not introduced. This method retained the organized structure of the spectrum and included it in the nearshore wave transformations by using a parametric representation of the offshore wave climate. Hasselmann et al. (1973, 1976) give good descriptions of the use of parametric models for wave generation and propagation. The principles in this case were quite similar.

12. The separation of the deepwater wave records into swell and wind-sea permits distinctly different approaches to the treatment of the frequency and directional characteristics of these wave populations. Swell that has propagated beyond its area of generation usually contains almost all of its energy in a narrow frequency and direction band. Thus, swell can be adequately described as a unidirectional, monochromatic wave train impinging on a coast. On the other hand, the local wind-sea tends to have a distinct shape

in frequency and is quite broad banded in direction space. Therefore, two formulations are imposed on the description of the deepwater wind-sea energy levels. The frequency spectrum is characterized by the form given by Kitaigorodskii (1962), and a cosine⁴ ($\theta - \bar{\theta}$) distribution of energy for deepwater input conditions to the Phase III parametric spectral form where $\bar{\theta}$ is the central angle of the spectrum.

13. Both populations of wave energy can be represented by three parameters: wave height H , wave period T , and wave direction θ for the unidirectional monochromatic swell and α_{sea} (Kitaigorodskii's equilibrium range constant) f_{sea} and θ_{sea} for the local wind-sea where f_{sea} is a characteristic frequency associated with the spectrum. For consistency, if a period is defined as $T_{sea} = 1/f_{sea}$ and the integral form of the energy density spectrum is used to obtain a wave height H_{sea} , as a function of α_{sea} and f_{sea} , then both the swell and wind-sea can be described by comparable parameters, namely H_{mo} , T , and θ . It should be recognized that this by no means restricts the local wind-sea to unidirectional monochromatic waves, but rather only to a fixed deepwater spectral shape. A 2-D spectrum describing the deepwater wind-sea contribution from the Phase II estimates was constructed (from α_{sea} , f_{sea} , and θ) and transformed by frequency and directional components to a 10-m water depth. Changes in the spectral form were based on shoaling, refraction, nonlinear wave-wave interactions, and surf-zone breaking. The swell component was transformed as a single frequency and direction using similar mechanisms.

14. One of the primary motivations for performing the Phase II calculations as an intermediate step between the Phase I hindcast and the Phase III nearshore wave transformations was to provide a better representation of the effects of the geometry of the coastline on wave generation near the Atlantic coast. This was carried through in more detail during the Phase III process, where nearshore sheltering was employed. The amount of wave sheltering (or the selection of the sheltering angle) depends upon the location of the input Phase II station, relative to the given Phase III station being considered, and the shoreline. Since the WIS Phase III reports are intended only to serve as general summaries of the wave conditions along the entire length of a 16-km shoreline segment, only first-order shoreline orientations were considered, namely the shoreline angle along the 16-km reach (Jensen 1983a).

15. The Phase III hindcasts were generated every 3 hr for the entire 20-year record. The information included significant heights, mean periods,

and mean directions for sea and swell. A combined height, period, and direction are also calculated. The combined wave height is equal to the square root of the sum of the squares of the wind-sea and swell heights. If the transformed wind-sea height is greater than the swell height, then the period and direction from the wind-sea component are selected rather than that for the swell, and vice versa.

16. The wave period determined for the WIS estimates is a weighted average wave period \bar{T}_{WIS} determined from the spectrum as:

$$\bar{T}_{\text{WIS}} = \frac{1}{\bar{f}}$$

and

$$\bar{f} = \frac{\int_0^{\infty} f E(f) df}{\int_0^{\infty} E(f) df} \quad (1)$$

where

\bar{f} = weighted average frequency

f = frequency

$E(f)$ = spectral density function

17. For this investigation, Phase III Station 81 (36.25° N, 75.71° W) was used. The beach was considered oriented parallel to a line 20 deg west of north.

FRF Measurements

18. The measurement program at the FRF provides two data sets that can be compared with the hindcasted wave estimates for the adjacent coast. The first consists of 5 years of energy spectra from a Waverider buoy located in a depth of 8.5 m.

19. The Waverider gage measures the vertical acceleration produced by the passage of a wave. The acceleration signal is doubly integrated to produce a displacement signal, which is transmitted by radio to an onshore receiver. Wave amplitudes, according to the manufacturer's specifications, are correct to within 3 percent of their actual value for wave frequencies between 0.065 and 0.500 Hz (corresponding to 15- to 2-sec wave periods). The buoys were calibrated semiannually to ensure that the integrity of the measuring device adhered to the manufacturer's specification.

20. Data were routinely collected every 6 hr except during storms, when hourly data were obtained. However, to ensure that the data collected more often during high wave conditions did not bias the statistics, a subset of the available data was selected every 6 hr near 0100, 0700, 1300, and 1900 Eastern Standard Time. The 6-hr measurement interval provides an unbiased representation of the variation of the wave climate throughout the day, as do the hindcasts made every 3 hr. A data record consisted of 4,096 points recorded at 0.5 Hz for approximately 34 min. The time series were quality controlled, and erroneous values, although uncommon, were edited. After application of a 10-percent cosine bell data window, an ensemble-band-averaged variance (energy) spectrum was computed using a Fast Fourier Transform with a 0.0117 Hz (3/256 sec) band width and 64 deg of freedom.

21. The wave height H_{mo} determined from the free-surface measurements was defined as four times the square root of the total variance of the free surface, where the total variance σ^2 is:

$$\sigma^2 = \sum_1^n H(f_i) \Delta f \quad (2)$$

where

$H(f_i)$ = discrete spectral density function

f_i = component frequency

n = number of bands

Δf = frequency band width

The peak spectral wave period T_p is the inverse of f_m where f_m is the center frequency of the spectral band that contained the maximum spectral density.

22. The second data set was obtained from a directional gage consisting of a 250-m-long linear array of pressure transducers installed in 1986 1 km from shore in a depth of 8.5 m. Details of the gage components and analysis technique are presented by Long and Oltman-Shay (in preparation). One year of measured wave directions obtained from the linear array was compared with the WIS direction estimates. The direction associated with the peak of the measured directional spectrum was used for comparison with the WIS dominant direction.

PART III: COMPARISON OF WIS TO FRF

Percent Occurrence Tables

23. Included in the WIS Phase III Atlantic coast hindcasts (Jensen 1983a) are 20-year azimuth and 20-year all-direction tables. The azimuth tables give the percent occurrence of waves in height and period ranges for 30-deg direction intervals. Only wave directions with a component toward shore are considered. The all-direction tables present the distribution of heights and periods independently of direction. For the discussion that follows, the table for all directions will be used; use of the azimuth tables is demonstrated in Part IV to estimate a longshore sediment transport rate.

24. The wave period ranges are in 1-sec intervals (except for the first increment where the range is from 0 to 2.9 sec and the last increment where the range is all periods greater than 19.0 sec). The height ranges are in 0.5-m increments. The percent occurrence values have been multiplied by 100 to allow more accuracy with less printing space. Summations across rows and columns are provided in the last row and column of each table.

25. As can be seen in Table 1 for the WIS estimates and Table 2 for the FRF measured data, the two distributions are quite different. Table 3 shows the difference between the actual percent occurrence values when the measured distribution is subtracted from the WIS distribution. Upon comparison, it is clear that not only are the distributions different for long periods, but that there is a concentration of WIS values with heights under 0.5 m and periods less than 7 sec which does not appear in the measured data. To investigate the details of these differences, the summations in the last rows and columns in Tables 1 and 2 were compared.

Wave Period

26. The summations in Tables 1 and 2 provide a convenient way to summarize the wave periods when used in the form of wave period histograms. Figure 3 shows a histogram of the WIS estimates versus FRF measured wave periods. Although the shape of the WIS distribution is similar to the distribution of the measured data, the WIS estimates have a maximum at 3 to 5 sec (with a secondary peak at 7 sec), as compared with the peak at 8 to 9 sec for the gage measurements. These distributions vary because the wave period used to

Table 1
Percent Occurrence of Wave Heights and Periods for WIS Estimates

HEIGHT,M	ANNUAL PERCENT OCCURRENCE(X100) OF HEIGHT AND PERIOD																	TOTAL
	PERIOD,SEC																	
	1.0- 2.9	3.0- 3.9	4.0- 4.9	5.0- 5.9	6.0- 6.9	7.0- 7.9	8.0- 8.9	9.0- 9.9	10.0- 10.9	11.0- 11.9	12.0- 12.9	13.0- 13.9	14.0- 14.9	15.0- 15.9	16.0- 16.9	17.0- 17.9	18.0- 18.9	
0.00 - 0.49	646	1405	1177	1067	512	394	97	18	34	12	13	5	5380
0.50 - 0.99	.	220	888	483	196	410	150	13	63	91	5	2519
1.00 - 1.49	.	.	63	359	183	275	93	20	61	60	1	1115
1.50 - 1.99	.	.	.	26	141	235	63	19	36	9	529
2.00 - 2.49	32	157	68	16	22	8	303
2.50 - 2.99	17	49	24	10	2	1	103
3.00 - 3.49	4	22	8	1	35
3.50 - 3.99	2	8	1	1	12
4.00 - 4.49	1	1	1	3
4.50 - 4.99	1	1
5.00 - 5.49	0
5.50 - 5.99	0
6.00 - 6.49	0
6.50 - GREATER	0
TOTAL	646	1625	2128	1935	1064	1488	524	134	243	185	23	5	0	0	0	0	0	0

Table 2
Percent Occurrence of Wave Heights and Periods for FRF Measured Data

HEIGHT,M	ANNUAL PERCENT OCCURRENCE(X100) OF HEIGHT AND PERIOD																	TOTAL	
	PERIOD,SEC																		
	1.0- 2.9	3.0- 3.9	4.0- 4.9	5.0- 5.9	6.0- 6.9	7.0- 7.9	8.0- 8.9	9.0- 9.9	10.0- 10.9	11.0- 11.9	12.0- 12.9	13.0- 13.9	14.0- 14.9	15.0- 15.9	16.0- 16.9	17.0- 17.9	18.0- 18.9		19.0- LONGER
0.00 - 0.49	14	38	34	58	94	222	546	504	213	178	178	90	85	79	14	.	.	27	2374
0.50 - 0.99	11	121	234	443	422	398	816	848	504	294	151	54	67	119	9	.	5	31	4527
1.00 - 1.49	.	14	113	303	331	220	238	299	182	135	97	18	7	13	5	.	4	22	2001
1.50 - 1.99	.	.	.	97	187	81	81	47	47	68	56	18	5	9	.	.	2	7	705
2.00 - 2.49	.	.	.	2	27	56	32	25	32	31	29	2	7	243
2.50 - 2.99	2	11	9	11	16	5	11	2	5	7	79
3.00 - 3.49	2	.	20	4	7	9	11	5	2	60
3.50 - 3.99	2	2	.	.	2	6
4.00 - 4.49	2	.	2	4
4.50 - 4.99	0
5.00 - 5.49	0
5.50 - 5.99	0
6.00 - 6.49	0
6.50 - GREATER	0
TOTAL	25	173	381	903	1063	990	1722	1754	1000	722	531	197	183	229	28	0	11	87	

Table 3
Difference Between WIS Estimates and FRF Measured
Percent Occurrence Tables

HEIGHT, M	ANNUAL DIFFERENCE (PERCENT X100) [WIS - FRF]																		TOTAL
	PERIOD, SEC																		
	1.0- 2.9	3.0- 3.9	4.0- 4.9	5.0- 5.9	6.0- 6.9	7.0- 7.9	8.0- 8.9	9.0- 9.9	10.0- 10.9	11.0- 11.9	12.0- 12.9	13.0- 13.9	14.0- 14.9	15.0- 15.9	16.0- 16.9	17.0- 17.9	18.0- 18.9	19.0- LONGER	
0.00 - 0.49	631	1367	1142	1009	418	172	-449	-486	-178	-166	-165	-85	-84	-79	-14	.	.	-27	3006
0.50 - 0.99	-10	99	653	40	-225	11	-665	-835	-441	-203	-146	-54	-66	-118	-9	.	-5	-30	-2004
1.00 - 1.49	.	-14	-50	56	-148	54	-145	-279	-121	-75	-96	-18	-7	-12	-5	.	-3	-21	-884
1.50 - 1.99	.	.	.	-71	-46	154	-18	-28	-10	-59	-55	-18	-5	-9	.	.	-1	-7	-173
2.00 - 2.49	.	.	.	-1	4	101	35	-9	-10	-22	-28	-1	-7	62
2.50 - 2.99	-1	5	40	13	-6	-3	-10	-1	-5	-7	25
3.00 - 3.49	-1	3	2	4	-6	-8	-10	-5	-1	-22
3.50 - 3.99	1	6	.	1	.	-1	7
4.00 - 4.49	1	-1	1	-1	0
4.50 - 4.99	0
5.00 - 5.49	0
5.50 - 5.99	0
6.00 - 6.49	0
6.50 - GREATER	0
TOTAL	621	1452	1745	1033	2	496	-1199	-1621	-755	-535	-506	-188	-180	-226	-28	0	-9	-85	

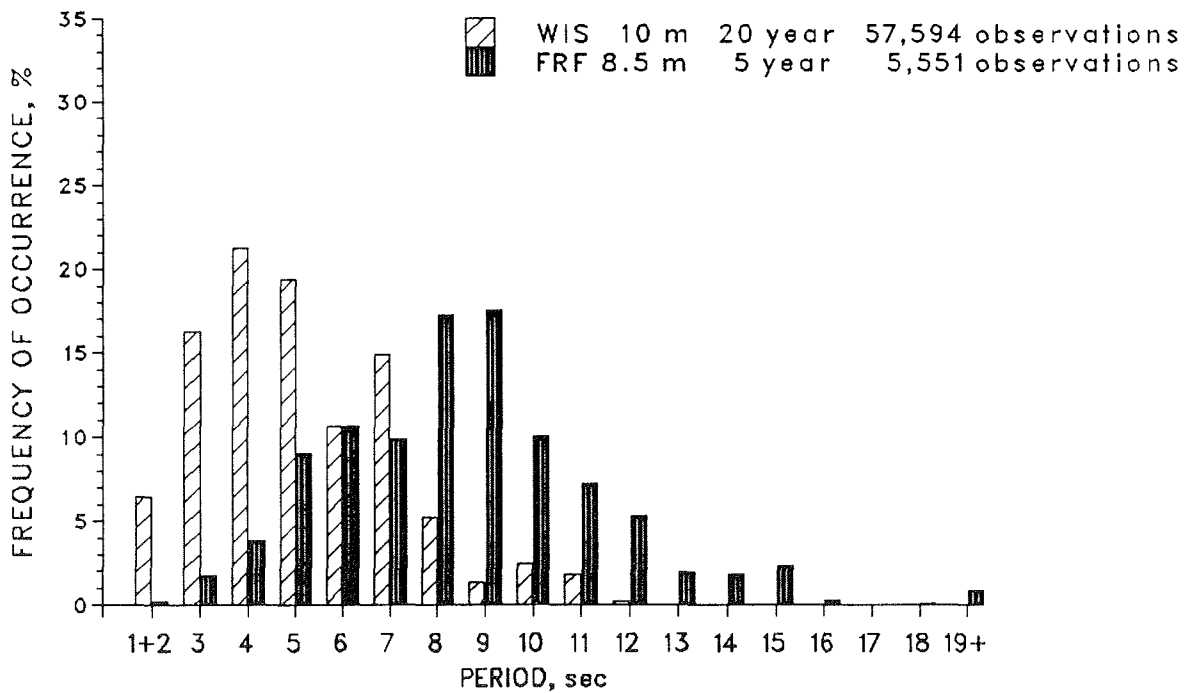


Figure 3. Histograms comparing WIS weighted average and FRF measured peak spectral wave periods

summarize the WIS estimates is not the same wave period that is computed for the measured data. An understanding of these differences is essential before the WIS estimates can be used with confidence.

27. The WIS definition (Equation 1) of peak wave period, as it is referred to in the Atlantic coast WIS Report 9 (Jensen 1983a), is not the same as the peak spectral wave period computed for the measured wave records. The WIS period \bar{T}_{WIS} more appropriately should be referred to as the weighted average wave period because of its inverse relationship to the weighted average frequency \bar{f} . Only if similar wave parameters are compared can an assessment be made of how consistent WIS estimates are with actual wave climate measurements.

28. In an effort to resolve this problem, a transformation between \bar{f} and f_m was derived as follows. The local sea portion of the spectrum under active growth $G(f)$ was defined by Kitaigorodskii's (1962) parametric representation:

$$\begin{aligned}
 G(f) &= \frac{\alpha g^2 f^{-5}}{(2\pi)^4} & f \geq f_m \\
 G(f) &= \frac{\alpha g^2 f_m^{-5}}{(2\pi)^4} e^{[1-(f_m/f)^4]} & f < f_m
 \end{aligned}
 \tag{3}$$

where

α = constant of spectrum

g = gravitational acceleration

In a discrete spectrum, \bar{f} (Equation 1) is determined by summing over all the frequency bands. After a variable transformation to f_i/f_m ($i = 1, 2, \dots, n$; n = number of spectral bands), substituting Equation 3 into Equation 1; summing the discrete form of Equation 1 piecewise from $0.0 \leq f_i/f_m < 1.0$ and $1.0 \leq f_i/f_m < 10.0$, and reducing, the following relationship results:

$$\bar{f} = \lambda f_m
 \tag{4}$$

where $\lambda = 1.14$. To transform the distribution of \bar{T}_{WIS} to a T_{WIS} peak wave period distribution, each \bar{f} was multiplied by $1/\lambda = 0.88$ and

inverted. Although this 12-percent correction could not be applied to the cases in Figure 3 where the swell wave period was selected, application to the 81 percent of the WIS estimates in which the sea was dominant improved the agreement as seen in Figure 4. The gap in the distribution at 4-sec periods in Figure 4 is artificial and due to transforming the periods that were saved only to whole numbers.

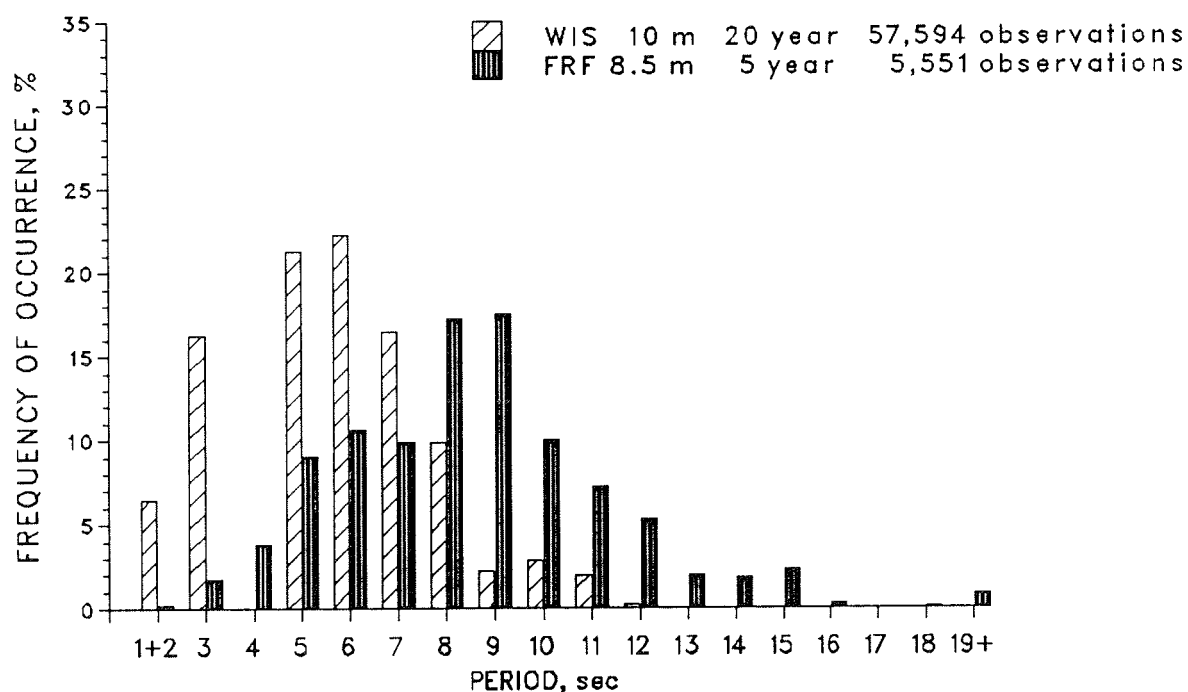


Figure 4. Histogram comparing peak spectral WIS and FRF measured periods

29. It is clear that the differences between the wave period distributions are not completely due to the different ways the wave periods values were determined. In fact, it would appear from Figures 3 and 4 that the improvement was small in comparison with the magnitude of differences that remain. The differences remain unexplained; however, most of the explanations are areas of active research where the questions about wave generation and propagation are as yet unresolved. Some considerations are as follows (Jensen 1983a).

. . . the Phase III wave characteristics were generated from a different type of procedure common to the Phase I and II computations. Phase I and II wave characteristics were generated from a numerical wave model which simultaneously propagated and transformed the data over a discrete grid. This approach could not be employed for the evaluation of the nearshore

wave characteristics because of its relative computational costs; but more importantly, the transforming mechanisms [refraction, shoaling, wave-wave interactions, bottom friction, high frequency dissipation, percolation, etc.] within finite water depths have not been clearly defined in terms of their importance to the changes in wave conditions.

In fact, no additional wave growth is permitted over the 50-km distance from the Phase II to Phase III stations. Wave generation does occur in finite water depths, and nonlinear wave-wave interactions tend to move the spectral peak toward lower frequencies during active wave growth. Consequently, the WIS estimates are biased toward shorter periods.

30. The WIS technique also propagates the two wave populations, swell and sea, to shore independently. However, the present understanding of the depth-controlled breaking mechanisms between two independent wave populations is still as yet an unresolved topic of research. Recent work by Vincent and Smith (in press) has shown that the dissipation of a higher frequency wave train in the presence of a lower frequency wave train is much more rapid than the dissipation without the lower frequency wave train present. This phenomenon, if taken into account, would also tend to influence the distribution of wave periods in such a way to make periods longer, which would improve the agreement with the measured distribution of wave periods.

31. Finally, it is important to remember that WIS estimates synoptic-scale climatological conditions for a range of coastline 16 km long. A gage provides wave characteristics for the specific location where the measurements are made. Idiosyncracies of the gage location, although not considered to have a large effect, could produce variations from the WIS estimates.

32. If a spectrum from gage measurements or a model estimation, is available, either the average or peak wave period can be readily calculated. One drawback with using the weighted average period is that it can fall between the dominant periods in a multiple peak spectrum and thus not be associated with any wave population present. In addition, engineering guidance such as that found in the Shore Protection Manual (SPM) (1984), generally uses the peak wave period (or something closely related) as opposed to an average period.

33. Computations were performed to see how well the WIS estimates compared with a weighted average wave period computed from the measured data \bar{T}_{FRF} . Figure 5 shows that the \bar{T}_{WIS} and \bar{T}_{FRF} distributions agree quite

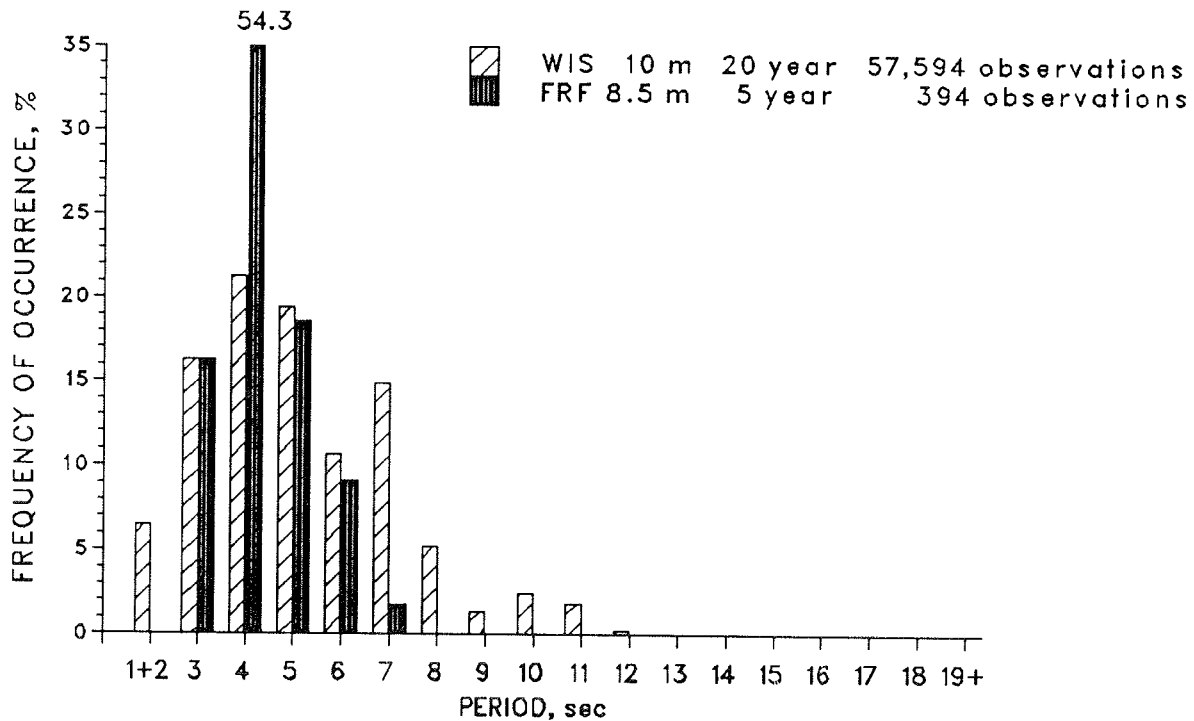


Figure 5. Histogram comparing weighted average WIS and FRF measured periods

well. Although the agreement is good, it is not conclusive because the constraints on the measured data necessary to compute a reasonable weighted average period that could be associated with the wind sea or the swell in a measured spectrum greatly reduced the number of cases. The best that could be expected was to model the wind sea, which resulted in the following constraints:

- a. The sea portion of the spectrum was selected by specifying a low-frequency cutoff corresponding to the component celerity that was less than the wind speed; i.e. active wave growth conditions were required.
- b. The sea portion of the spectrum (below f_m) was differentiated from the swell by modeling that portion using the FRF spectral model (Miller and Vincent 1990).
- c. Only cases were considered that had a sufficient number of frequencies above the low-frequency cutoff to fit the model.

34. To this point, it has been shown that because of the use of different definitions, the WIS wave period estimates do not agree well with the measured wave period distributions. In addition, there does not appear to be an easy way to transform the WIS summaries to peak spectral wave period summaries. However, the utility of the WIS estimates is still very large, as demonstrated in the following section on wave height.

Wave Height

35. Figure 6 shows the WIS estimated and FRF measured wave height distributions displayed in cumulative form. The intersection of any point on the

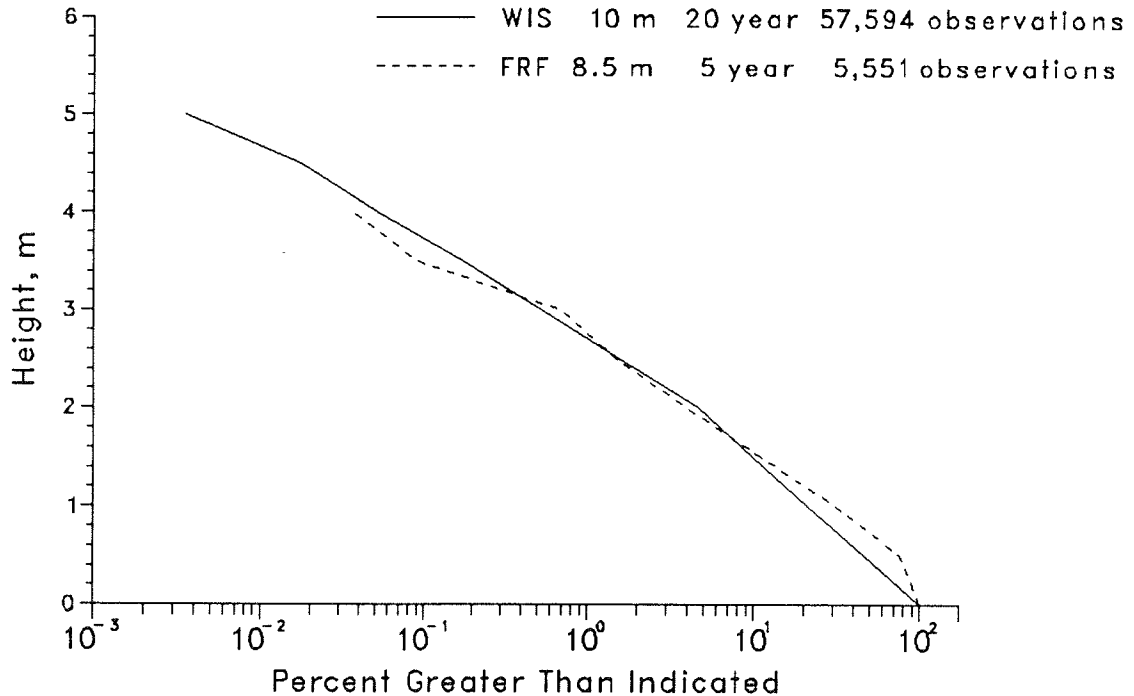


Figure 6. Comparison of WIS estimates and FRF measured cumulative wave height distributions

curve with the abscissa represents the percentage of the total number of observations that exceed the given height value on the ordinate. Although similar, there are some differences. The primary difference is that there are more low waves for the WIS estimates; for example, 44 percent of the heights exceed 0.5 m for the WIS distribution versus 76 percent for the FRF data. Likewise, 21 percent exceed 1 m for WIS, while 31 percent for the FRF. For waves heights over 2.0 m, on the other hand, the distributions are similar with a slight tendency for the WIS estimates to be higher.

36. The differences in depth between the 10-m WIS estimates and the measurements in 8.5 m have only a small effect. Considering linear shoaling of a monochromatic 10-sec wave, for example, the height could be expected to be 2.4 percent greater at the gage site located in 8.5 m of water versus at the 10-m depth for the WIS estimates. This amounts to only a 10-cm difference in a 4-m wave height.

37. Use of the 5-year measurement data set allows the height distribution to be determined to a probability of only 0.1 to 0.01 percent. Using the 20-year WIS estimates, the wave height distribution can be reasonably well determined to a probability level of 0.01 to 0.001 percent. Unfortunately, for most engineering designs, the probability level of interest is usually in the range of 10^{-5} to 10^{-6} . Such a range corresponds to a risk of 5 to 10 percent that the selected wave height will not be exceeded within a 40- to 50-year period (Wang and Lé Mehauté 1983). Although there are different methods for extrapolating a given probability distribution to low probability levels, it is sufficient to say that the engineer must use any such estimate with caution. The similarity of the distributions is encouraging and suggests that the WIS estimates provide a very useful tool for design purposes. In this case, the engineer may be more comfortable using the longer term WIS estimates since they can be used with some confidence to extrapolate to lower probability levels and are more conservative.

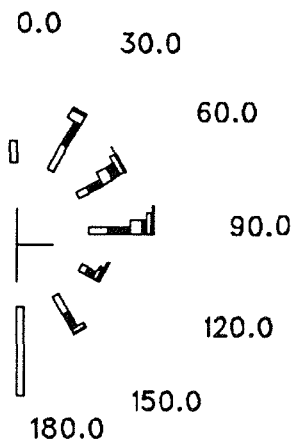
Wave Direction

38. In this section, the directional distributions of wave data are presented as wave roses such as those in Figure 7. These wave roses include the 30-deg resolution used in the azimuth tables, which differs from the 45-deg roses presented in WIS Report 9 (Jensen 1983a). The petal angle is the mean angle of the direction interval; the length of each segment of the petal is proportional to the occurrence frequency of the waves; and the width is proportional to the wave height.

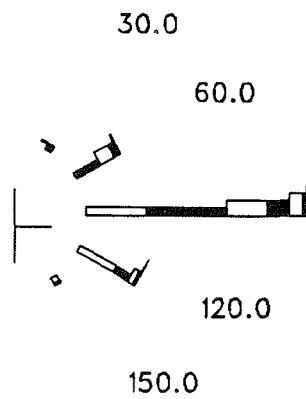
39. The difference in the cumulative height distributions is due to the high percentage of low waves from the south near shore-parallel, shown in Figure 7 for the WIS estimates. In general, however, the WIS directions were distributed over all of the eight-onshore compass directions with a tendency for waves over 2 m being directed more shore-normal.

40. In comparison, the 1-year measurement (beginning September 1986 and ending August 1987) shows the measured directions to be more shore-normal, with few shore-parallel measurements. However, for wave heights over 2 m, both the WIS estimated and FRF measured distributions tend to show that the waves are directed near shore-normal.

41. Again insight is possible when the differences in the WIS estimates and the FRF measured data are examined. Swell, with longer wave lengths than



WIS Estimates
Height 0.5 m
Direction 60 deg



Linear Array
Height 0.9 m
Direction 69 deg

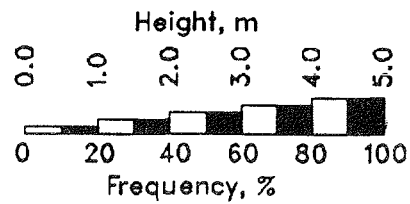


Figure 7. Wave rose diagram comparing WIS and linear array information

wind sea, is more likely to be shore-normal due to refraction. The WIS estimates tend to be distributed more evenly across all directions than the measured data. This may be due to how the WIS hindcast represents the swell as a single spectral line and the choice between two directions based on whether the sea or swell contain the dominate amount of spectral energy. Thus, the direction of the sea portion of the spectrum, which generally contains more energy even shortly after wave generation begins and tends not to be shore-normal, is chosen more often.

42. Another reason for the difference is that WIS neglects coastal features, such as shoreline variation, smaller than the 16-km reach used in Phase III calculations. The difference arises because wave generation in very shallow water within 1 km of shore at the wave gage site (particularly for winds blowing parallel with the shoreline) is very different from wave generation 50 km from shore at the Phase II location.

Summary

43. The mean wave periods computed for the WIS estimates should not be considered interchangeable with the peak spectral wave periods computed for the FRF measured data. After transforming the WIS mean wave periods to peak wave periods, for the active growth cases, it appears there may have been a problem with the hindcast technique that results in the periods being underestimated. The wave height values are in close agreement for wave heights above 1 m. The WIS wave directions are more evenly distributed in comparison with the 1 year of measurements. To ascertain whether the long-term WIS estimates or short-term FRF measurements will provide the engineer the better results is difficult as long as there are not sufficiently long measurement programs along the US coastline.

PART IV: LONGSHORE SEDIMENT TRANSPORT ESTIMATE

44. For many coastal engineering problems, an estimate of the longshore sediment transport rate is desired. In this section, the WIS estimates and the linear array measurements are used to compute a transport rate for the FRF. Estimating the longshore sediment transport rate is simply an example of the type of uses for the WIS wave information. The important thing is to see how consistent the estimated values are despite the differences between the WIS estimates and FRF measurements. Confidence in using the WIS summaries should be reinforced where the results are consistent.

45. Gravens (1988) presents a procedure for using the 20-year percent occurrence azimuth tables. This procedure is used to estimate longshore sediment transport rates under the assumptions of straight and parallel bottom contours. Refraction and shoaling of linear waves are calculated using Snell's law for wave direction and the equation of conservation of wave energy flux for wave height. A shallow-water wave breaking criterion defines wave properties at the break point, and longshore sediment transport rates are calculated by means of the energy flux method of the SPM (1984). The volumetric longshore sediment transport rate Q (m^3 per year) is given by

$$Q = \frac{KP_{1s}}{(\rho_s - \rho)g(1 - a)} \quad (5)$$

where

K = nondimensional empirical coefficient, $K = 0.77$

P_{1s} = longshore wave energy flux factor at breaking

ρ_s = density of sediment (quartz sand)

ρ = density of water

g = acceleration of gravity

a = porosity of beach sediment, $a = 0.4$

Replacing P_{1s} in Equation 5 with its analytical equivalent from linear wave theory (SPM 1984, Equation 4-39) yields

$$Q = \frac{K}{16(\rho_s/\rho - 1)(1 - a)} \frac{\sqrt{g}}{\sqrt{\gamma}} \frac{H_b^{5/2}}{2.386} \sin(2\alpha_b) \quad (6)$$

where

H_b = breaking wave height

γ = 0.78 is the breaker index

α_b = breaking wave angle

The factor 2.386 converts the input significant wave height to root mean square wave height for compatibility with the $K = 0.77$ design value.

46. The computation procedure consisted of first estimating a period value for each height band of each of the direction bands. These average period values are determined using a weighting function that tends to emphasize the periods that occur most often. The center of the 0.5-m height bands and the 30-deg direction bands was chosen as the representative values. With the average height, period and direction, water depth (10 m for Phase III), and percent occurrence, Q is estimated. The total annual rate, determined by summing the contribution for all heights within all angle bands, is given in Table 4.

Table 4
Estimated Longshore Sediment Transport
Rate, m³/year

<u>Direction</u>	<u>Transport Rate</u>	
	<u>WIS Estimate</u>	<u>FRF Measurements</u>
Southward	980,000	1,280,000
Northward	-380,000	-730,000
Net	600,000	550,000

47. Percent occurrence tables for the linear array data were generated using the same height, period, and direction bands. The resulting estimated longshore sediment transport rate is also given in Table 4. In comparison with the WIS estimates, the gross southward and northward values were 23 and 48 percent larger, respectively. However, the estimated net longshore sediment transport rate differs by only 8 percent.

48. Because the linear array data are only from 1 year, annual WIS sediment transport rate estimates are presented in Table 5 along with the mean and standard deviation of the gross southward, northward, and net values for comparison. The measured southward transport value is within 1 standard deviation of the annual mean WIS value. The measured northward value is not; however, it is well within the range of annual values estimated for the 20-year interval.

Table 5
Annual Sediment Transport Rates
Using WIS Estimates (m³/year)

<u>Year</u>	<u>Southward</u>	<u>Northward</u>	<u>Net</u>
1956	1,284,000	-648,000	636,000
1957	820,000	-301,000	519,000
1958	866,000	-853,000	13,000
1959	803,000	-175,000	628,000
1960	1,072,000	-304,000	768,000
1961	875,000	-409,000	466,000
1962	1,942,000	-400,000	1,542,000
1963	903,000	-329,000	574,000
1964	860,000	-820,000	40,000
1965	713,000	-281,000	432,000
1966	758,000	-430,000	328,000
1967	976,000	-217,000	759,000
1968	725,000	-171,000	554,000
1969	1,298,000	-290,000	1,008,000
1970	780,000	-474,000	306,000
1971	835,000	-553,000	282,000
1972	1,371,000	-371,000	1,000,000
1973	1,076,000	-301,000	775,000
1974	649,000	-154,000	495,000
1975	1,109,000	-250,000	859,000
Mean	986,000	-386,000	599,000
Standard Deviation	305,000	199,000	352,000

49. Despite the differences between the WIS hindcasts and FRF measurements, for this application the 20-year WIS estimated longshore sediment transport rate seems reasonable and may provide better engineering guidance than a single-year estimate based on wave measurements. However, the reason for this is that the sediment transport Equation 6 is not particularly sensitive to wave period. Differences in wave height and wave direction, for which the WIS hindcasts and FRF measurements generally agree for all but the lowest waves, have a much larger effect on the estimated sediment transport rate. A comparison of the effect of each parameter on the estimated transport rate is shown below:

Height <u>m</u>	Period <u>sec</u>	Direction <u>deg</u>	Depth <u>m</u>	Frequency of Occurrence, %	Variable Diff., %	Rate <u>m³/yr</u>	Q Diff., %
1.25	6.5	45	10	3.07	--	100,000	--
1.25	<u>8.5</u>	45	10	3.07	+31	116,000	+ 16
1.25	6.5	<u>15</u>	10	3.07	-66	55,000	- 45
<u>1.75</u>	6.5	45	10	3.07	+40	2,287,000	+127
1.25	6.5	45	<u>8.5</u>	3.07	-15	104,000	+ 4
1.25	6.5	45	10	<u>4.00</u>	+30	131,000	+ 31

The first row was selected at random from the computations used to produce Table 4. It should be noted that:

- a. The direction is the direction from shore-normal where smaller values are closer to shore-normal.
- b. The percent occurrence is related to the proportion of time that these conditions were expected to occur during any given year.
- c. Variable-difference was determined as the ratio of the value underlined to the value in row 1.
- d. The Q-difference is the computed annual rate divided by the annual rate in the first row.
- e. Values underlined are intended simply to emphasize the variable for which the difference is attributed.

Clearly wave height and direction have a larger effect on the rate than wave period. Wave period does have a 16-percent effect, however, primarily because of its importance in refracting and shoaling the wave information into the breaking depth.

50. Comparing the transport rates computed from the WIS estimates with the measured data highlights the trade-off the engineer faces. The WIS estimates provide an advantage insofar as the 20 years of wave information reduce the chance that the sample is atypical of the wave climate at a given

location. However, while the gage measurements may provide more accurate wave information, these short-term measurements may not represent the true wave climate. For estimating longshore sediment transport rate, it appears that the 20 years of height and direction information provide a reasonable estimate, even though the period values are suspect. It should be noted that this is but one example at one site. Other applications may compare more or less favorably depending upon the sensitivity of the computations to the various wave parameters.

PART V: SUMMARY

51. After a description of the Atlantic coast Phase III WIS estimates and the FRF measurements data, wave period, height, and direction summaries were compared. The wave periods did not compare well, whereas the wave heights did. Comparison of wave directions was less conclusive; however, net longshore sediment transport estimates were very nearly the same. The utility of this study is in the belief that a better understanding of the Atlantic coast WIS hindcasts will help ensure the appropriate application of the WIS wave information.

52. In an attempt to reconcile differences in the wave period distributions, it was shown that the WIS weighted average period is different from the peak spectral period determined for the measured data. One disadvantage of using a weighted average period is that the period may not be associated with any wave train present. A variable transformation from weighted average to peak period was unsuccessful in resolving the majority of the differences. Other reasons were presented for the differences, suggesting that the problem is in the fundamental understanding of wave generation and transformation toward shore.

53. Wave height distributions compared well for values greater than 1 m. However, there was a difference for wave heights below 0.5 m. The percentage of WIS estimates was approximately twice as large as for the FRF measurements. Most of the 56 percent of WIS estimated wave heights below 0.5 m were directed near shore-parallel. This was in contrast with the linear array data, which were predominantly shore-normal because of small-scale coastal features that effectively reduced the fetch for shore-parallel winds.

54. Longshore sediment transport rate estimates were computed to investigate the consistency between using the WIS estimates versus the FRF measurements for engineering applications. Comparing an annual rate based on the 20-year WIS estimates with the rate estimated from 1 year of FRF measurements showed the net values to be very similar, whereas the gross northward and southward values differed by as much as a factor of 2. However, when annual values were computed for each of the 20 years of WIS hindcasts, the estimated gross transport rates based on FRF measured data fell well within the range of WIS values. The consistency in the WIS estimates was due in part to the transport rate computation being more sensitive to wave height and angle, for

which WIS estimates and FRF measurements generally agree for all but the lowest wave conditions, versus wave period for which the WIS estimates appear to be approximately 2 sec low.

55. It is recommended that the WIS hindcasts be used when long-term wave height and direction information is required. Wave period information may be misleading. However, as demonstrated for sediment transport rate, which is not highly sensitive to wave period, the WIS information appears quite useful. Other applications of the WIS hindcasts should include a sensitivity analysis and checks with measurements if possible.

56. It is important to note that the Atlantic coast WIS hindcasts were the first in the series of WIS hindcasts that now include all the US coasts. At present, the WIS hindcasts use a definition of wave period more consistent with the peak spectral wave period. As the understanding of wave generation and transformation has advanced, improvements have been incorporated into the hindcast model. In addition, considerable emphasis is being placed on comparison and verification of the WIS hindcasts with measurements. All of the Atlantic coast stations were hindcasted using the most up-to-date WIS techniques. This 1-year, 1988, hindcast was compared on a case-by-case basis with offshore and inshore gage measurements from New England to Florida. The results, which will be published in 1991, show very good agreement.

57. Until long-term directional wave measurements are available for shallow-water locations along all of the US coasts, the WIS hindcast results remain one of the most valuable resources available to the coastal engineer. Where the luxury of both WIS and nearshore wave measurements are available, the engineer should use both to take advantage of the statistical stability of the 20-year hindcasts and the accuracy of the measurements.

REFERENCES

- Corson, W. D., and Resio, D. T. 1981 (May). "Comparisons of Hindcast and Measured Deepwater Significant Wave Heights," WIS Report 3, US Army Engineer Waterways Experiment Station, Vicksburg, MS.
- Corson, W. D., et al. 1981 (Jan). "Wave Information Studies of U. S. Coastlines; Atlantic Coast Hindcast, Deepwater, Significant Wave Information," WIS Report 2, US Army Engineer Waterways Experiment Station, Vicksburg, MS.
- Gravens, M. B. 1988. "Use of Hindcast Wave Data for Estimates of Longshore Sediment Transport," Symposium on Coastal Water Resources, American Water Resources Association, pp 63-72.
- Hasselmann, K., et al. 1973. "Measurements of Wind-Wave Growth and Swell Decay During the Joint North Sea Wave Project (JONSWAP)," Dtsch. Hydrogr. Z., A8(12).
- _____. 1976. "A Parametric Wave Prediction Model," Journal of Physical Oceanography, Vol 6, pp 200-228.
- Hemsley, M. 1986. "Field Wave Gaging Program," Proceedings West Coast Regional Coastal Design Conference, Oakland, CA, Nov 7-8 1985, pp 84-93.
- Jensen, R. E. 1983a (Jan). "Atlantic Coast Hindcast, Shallow-Water, Significant Wave Information," WIS Report 9, US Army Engineer Waterways Experiment Station, Vicksburg, MS.
- _____. 1983b (Sep). "Methodology for the Calculation of a Shallow-Water Wave Climate," WIS Report 8, US Army Engineer Waterways Experiment Station, Vicksburg, MS.
- Kitaigorodskii, S. A. 1962. "Applications of the Theory of Similarity to the Analysis of Wind-Generated Wave Motion as a Stochastic Process," Bulletin of the Academy of Science, USSR Geophysical Services 1, pp 105-117.
- Long, C. E., and Oltman-Shay, J. M. "Directional Characteristics of Waves In Shallow Water," Technical Report in preparation, US Army Engineer Waterways Experiment Station, Vicksburg, MS.
- Miller, H. C. and Vincent, C. L. 1990. "FRF Spectrum: TMA With Kitaigorodskii's f^{-4} Scaling," Journal of Waterway, Port, Coastal and Ocean Engineering, American Society of Civil Engineers, Vol 116, No. 1.
- Miller, H. C., Militello, Adele, Leffler, Michael W., Grogg, William E., Jr., and Scarborough, Brian L. 1988 (Aug). "Annual Data Summary For 1986 CERC Field Research Facility," Technical Report CERC-88-8, US Army Engineer Waterways Experiment Station, Vicksburg, MS.
- Resio, D. T. 1981. "The Estimation of Wind-Wave Generation in a Discrete Spectral Model," Journal of Physical Oceanography, American Meteorological Society, Boston MA, Vol 11, No. 4, pp 510-525.
- Shore Protection Manual. 1984. 4th ed., 2 Vols, US Army Engineer Waterways Experiment Station, Coastal Engineering Research Center, US Government Printing Office, Washington DC.
- Thompson, E. F. 1977 (Jan). "Wave Climate at Selected Locations Along U. S. Coasts," Technical Report CERC-77-1, US Army Engineer Waterways Experiment Station, Vicksburg, MS.

Vincent, C. L. and Smith, J. M. "Shoaling and Breaking of Multiple Wave Trains on a Beach," Journal of Waterway, Port, Coastal and Ocean Engineering, American Society of Civil Engineers, in press.

Wang, S., and Lé Mehauté, B. 1983 (May). "Duration of Measurements and Long-Term Wave Statistics," Journal of Waterway, Port, Coastal and Ocean Engineering, American Society of Civil Engineers, Vol 109, No. 2, pp 236-249.